Benchmark for PID control of Refrigeration Systems based on Vapour Compression ⋆

Guillermo Bejarano *, **José A. Alfaya** *, **David Rodríguez** *, **Fernando Morilla** **, and **Manuel G. Ortega** *

* *Departamento de Ingeniería de Sistemas y Automática, Escuela Técnica Superior de Ingeniería, Universidad de Sevilla. Camino de los Descubrimientos, s/n. 41092-Seville (Spain) (e-mails:* {gbejarano, jalonso9, drgarcia, mortega}@us.es*).*

** *Departamento de Informática y Automática, Escuela Técnica Superior de Ingeniería Informática, UNED. C/ Juan del Rosal 16, 28040-Madrid (Spain) (e-mail:* fmorilla@dia.uned.es*).*

Abstract:
The Benchmark proposed for the 3rd IFAC Conference on Advances in Proportional-Integral-Derivative Control (PID'18) held in July 2017 is described. This facilitates researchers to test their recent developments in the design of PID controllers on a challenging control problem. The paper focuses on the control of refrigeration systems: the canonical vapour-compression cycle is first described and then the MIMO control problem selected for the Benchmark PID 2018 is addressed, where the cooling power (through the outlet temperature of the evaporator secondary fluid) is intended to be controlled, as well as the degree of superheating at the evaporator outlet, using the compressor speed and the expansion valve opening as manipulated variables. The control systems described in this paper are ready to test other multivariable control strategies, despite being focused on PID regulators. Full documentation about the Benchmark was linked on the website of PID'18 and it will remain in `http://www.dia.uned.es/~fmorilla/benchmarkPID2018/`.

Keywords: Vapour-compression refrigeration, Rankine cycle, Dynamic modelling, Decentralised control, PID control

1. INTRODUCTION

Refrigeration based on vapour compression is the leading technology worldwide in cooling generation, including air conditioning, refrigeration, and freezing. Controlling room temperature is involved in as widely diverse areas as human comfort, food storage/transportation, and industrial processes. Although in some cases air conditioning and refrigeration are separately considered, all these systems use the inverse Rankine cycle to remove heat from a cold reservoir (i.e. a cold storage room) and transfer it to a hot reservoir, normally the surroundings. A great deal of energy is required in such tasks, that affects negatively energy and economic balances. It is reported that approximately 30% of total energy over the world is consumed by Heating, Ventilating, and Air Conditioning (HVAC) processes (Jahangeer et al., 2011), while air conditioners and refrigerators represent 28% of home energy consumption in USA (Ruz et al., 2017). Furthermore, supermarkets and department stores are known to be one of the largest consumers in the energy field; the average energy intensity for grocery stores represents around 500 kW h/m^2 a year in USA, which means more than twice the energy consumed by a hotel or office building per square meter (Lukic, 2016). Considering commercial and residential buildings, around 45% of total electricity consumption is devoted to HVAC systems (Kalkan et al., 2012).

Refrigeration systems are closed cycles, whose components are connected through pipes and valves, which causes strong non-linearities and high coupling. This is why the dynamic modelling of such systems is not trivial matter. The most important elements are the heat exchangers, while the expansion valve, the compressor, and the thermal behaviour of the secondary fluids are usually statically modelled, since their dynamics are at least one order of magnitude faster than those of the heat exchangers.

There is an extensive literature related to control of refrigeration systems. To achieve high energy efficiency while satisfying the cooling demand, it must be taken into account that heat transfer at the evaporator is key for the overall efficiency. The highest efficiency would be achieved if the refrigerant at the evaporator outlet was saturated vapour. This ideal behaviour is not advisable nor applicable in practice, since the risk of liquid droplets appearing at the evaporator outlet is very high in transient, which must be definitely avoided because the evaporator outlet matches the compressor intake. Therefore, the approach conventionally applied in industry consists in operating the cycle with a certain degree of superheating of the refrigerant at the evaporator outlet (T_{SH}), which is defined as the difference between the refrigerant temperature at the

⋆ This work was supported by MCeI (Grant DPI2015-70973-R).

evaporator outlet and the saturation temperature at the evaporator pressure. Therefore, the conventional control scheme is very simple: in addition to the reference imposed by the cooling demand, a certain set point on the degree of superheating T_{SH} is applied. Then, the controller is designed to get these two variables to track their references in presence of disturbances, by manipulating the compressor speed and the expansion valve opening.

The main difficulty in controlling this process lies in high thermal inertia, dead times, high coupling between variables, and strong non-linearities. The most used linear techniques which can be found in the literature are decentralised PID control (Marcinichen et al., 2008; Salazar and Méndez, 2014), decoupling multivariable control (Shen et al., 2010), LQG control (Schurt et al., 2009), model predictive control (Ricker, 2010), and robust H_∞ control (Bejarano et al., 2015). The main advantage of using PID controllers is their ease of implementation and tuning, while the advantage of more advanced controllers is mainly their performance improvement.

The Benchmark PID 2018 provides a practical approach for researchers to address a stimulating control problem, which their recent developments in the design of PID controllers can be tested on. The intended audience is extended to undergraduate/ postgraduate students and also researchers who may be interested in testing novel control strategies on a validated model of an experimental plant. Other refrigeration benchmarks have been presented in the literature, regarding specific setups with on/off manipulated variables (Larsen et al., 2007; Ricker, 2010), while the proposed benchmark is focused on the most general refrigeration cycle, using a variable-speed compressor and an electronic expansion valve, in such a way that the manipulated variables are continuous, being inspired on the commercial software Thermosys (Alleyne et al., 2012). However, this benchmark provides an easy-to-use, fast testbed of the simplest refrigeration cycle that presents the intrinsic difficulties featuring this kind of systems.

This paper is organised as follows: the Refrigeration System and its control are stated in Section 2. The attention is first focused on the most general vapour-compression cycle; then the MIMO control problem selected for the Benchmark PID 2018 is exposed. Some details about the dynamic modelling are also given. Sections 3 and 4 describe how the test and comparative evaluation of multivariable PID controllers can be carried out using the files provided within the Benchmark. Finally, Section 5 summarises the conclusions. All the examples mentioned in this paper can be checked by downloading the files provided in the website: `http://www.dia.uned.es/~fmorilla/benchmarkPID2018/`. Full documentation about the Benchmark is also available on the website.

2. THE CONTROL OF REFRIGERATION SYSTEMS

2.1 Overview

A canonical one-compression-stage, one-load-demand refrigeration cycle is shown in Fig. 1, where the main components (expansion valve, compressor, evaporator, and condenser) are represented. The objective of the cycle is to remove heat from the secondary fluid at the evaporator and reject heat at the condenser by transferring it to the corresponding secondary fluid. The inverse Rankine cycle is applied, where the refrigerant enters the evaporator at low temperature and pressure and it evaporates while removing heat from the evaporator secondary fluid. The compressor increases the refrigerant pressure and temperature and it enters the condenser, where first its temperature decreases, secondly it condenses and finally it may become subcooled liquid while transferring heat to the condenser secondary fluid. The expansion valve closes the cycle by upholding the pressure difference between the condenser and the evaporator.

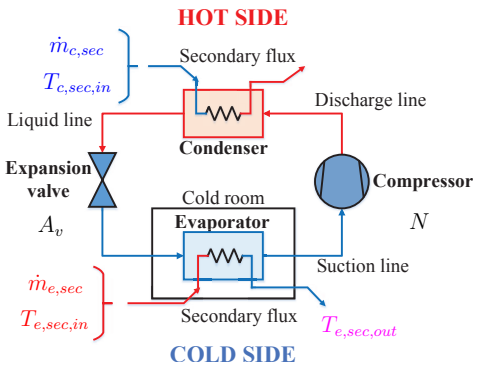

Fig. 1. Schematic picture of one-compression-stage, one-load-demand vapour-compression refrigeration cycle

The main control objective is to satisfy the cooling demand $\dot{Q}_e$. Furthermore, the desired cooling power is intended to generated as efficient as possible, which implies controlling the degree of superheating T_{SH}, as stated in Section 1. As widely known, energy efficiency is usually described in refrigeration field using the Coefficient of Performance (COP), which is defined as the ratio between the cooling power generated at the evaporator $\dot{Q}_e$ and the mechanical power provided by the compressor $\dot{W}_{comp}$.

In the Benchmark PID 2018 a particular application of refrigeration systems is considered. The cycle, working with R404a as refrigerant, is expected to provide a certain cooling power $\dot{Q}_e$ to a continuous flow entering the evaporator as secondary fluid, which is a 60% propylene glycol aqueous solution, whereas the condenser secondary fluid is air. Neither the mass flow $\dot{m}_{e,sec}$ nor the inlet temperature $T_{e,sec,in}$ of the evaporator secondary fluid are intended to be controlled. Therefore, the cooling demand can be expressed as a reference on the outlet temperature of the evaporator secondary fluid $T_{e,sec,out}$, where the mass flow and inlet temperature act as measurable disturbances. Regarding the condenser, the inlet temperature $T_{c,sec,in}$ and mass flow $\dot{m}_{c,sec}$ of the corresponding secondary fluid are also considered as disturbances. Thus, the only manipulated variables turn out to be the compressor speed N and the expansion valve opening A_v.

The system block programmed in Simulink® is represented in Fig. 2, where the manipulated variables, the controlled variables, and the disturbance vector are indicated, whereas Table 1 details the components of the disturbance vector. Note that the COP (Coefficient of Performance) is also included as a block output, despite not being a controlled variable but only an energy efficiency indicator.

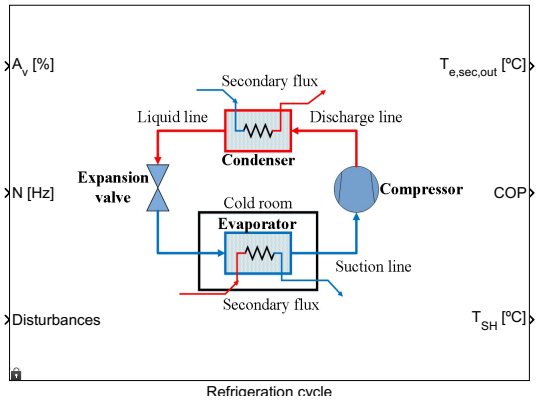

Fig. 2. Simulink® block showing the vapour-compression refrigeration cycle inputs and outputs

Table 1. Disturbance vector

Disturbance variable	Symbol	Unit
Inlet temperature of the condenser secondary fluid	$T_{c,sec,in}$	°C
Mass flow of the condenser secondary fluid	$\dot{m}_{c,sec}$	$g \cdot s^{-1}$
Inlet pressure of the condenser secondary fluid	$P_{c,sec,in}$	bar
Inlet temperature of the evaporator secondary fluid	$T_{e,sec,in}$	°C
Mass flow of the evaporator secondary fluid	$\dot{m}_{e,sec}$	$g \cdot s^{-1}$
Inlet pressure of the evaporator secondary fluid	$P_{e,sec,in}$	bar
Compressor surroundings temperature	T_{surr}	°C

2.2 About the controller

The multivariable controller needs to be an 11x2 Simulink® block, but it could be a continuous, discrete, or hybrid block. There is also total freedom to decide the structure of the block; the controller may use all input signals or some of them. The 11 input signals are: the outlet temperature of the evaporator secondary fluid $T_{e,sec,out}$, its reference, the degree of superheating T_{SH}, its reference, and the disturbance vector made up of the 7 variables indicated in Table 1. The two output signals (manipulated variables) are the expansion valve A_v and the compression speed N. A default multivariable controller has been programmed in the Benchmark PID 2018. It is a discrete decentralised controller, designed using affine parameterisation, where $T_{e,sec,out}$ is controlled by means of the expansion valve, while the compressor speed controls T_{SH}. Table 2 indicates the transfer functions used within the default controller, implemented with a sample time of 1 s. Note that the disturbance information is not used, thus it is a MIMO controller without feedforward compensation. More information regarding the default controller design is included in the Benchmark documentation linked in Section 1.

2.3 About the refrigeration system model

Different approaches can be found in the extensive literature about dynamic modelling of refrigeration systems. Most are focused on the heat exchangers, since their dynamics show to be dominant. One can find, from very detailed and complex models (e.g. the *finite-volume* approach, dating to MacArthur et al. (1983)), to simplified

Table 2. Discrete transfer functions used within the default controller

Controller pairing	Transfer function
$\{T_{e,sec,out}, A_v\}$	$\frac{-1.0136 - 0.0626z^{-1} + 0.9988z^{-2}}{1 - 1.9853z^{-1} + 0.9853z^{-2}}$
$\{T_{SH}, N\}$	$\frac{0.42 - 0.02z^{-2}}{1 - z^{-1}}$

ones oriented to the design of multivariable control strategies. That is the case of the *switched moving-boundary* (SMB) approach (Li and Alleyne, 2010; Alleyne et al., 2012), which divides the heat exchanger into a number of zones corresponding to different refrigerant states: superheated vapour, two-phase fluid, and/or subcooled liquid. The zone lengths are state variables, and different representations of the heat exchanger model (*modes*) are defined depending on the existence or absence of each zone. In the Benchmark PID 2018 the SMB approach has been selected to model the refrigerant behaviour when circulating through the heat exchangers, due to its ability to adapt to different systems and its better trade-off between accuracy and computational load. Nevertheless, some assumptions have been made to reduce even more the order of the original SMB model and therefore its complexity (Bejarano et al., 2017).

First, progressive replacement of environment-unfriendly refrigerants and rising costs of raw material have motivated changes in evaporator design, seeking low internal volume (Rasmussen and Larsen, 2011). As a result, the evaporator dynamics become faster and, if compared to typical condenser dominant time constant, they can be disregarded without too much loss of accuracy, thus the evaporator may be statically modelled and the condenser dynamics become dominant. Secondly, the refrigerant mass flow equilibrium between the condenser inlet and outlet is very fast compared to the heat transfer dynamics, therefore a unique refrigerant mass flow may be assumed, disregarding the fast transient due to mass flow imbalance.

Considering all these simplifications, the state vector of the whole cycle is reduced to that corresponding to the condenser. Moreover, when a subcooled liquid zone exists, the intrinsic dynamics of the state variables related to the superheated vapour zone and the two-phase zone can be disregarded due to density difference, which implies faster dynamics when compared with the dominant ones related to the subcooled liquid zone. When the latter is inactive, only the intrinsic dynamics of the state variables related to the superheated vapour zone are disregarded, as well as the states related to the subcooled liquid zone.

The simplified SMB model has been developed in Simulink® including constrained ranges for the inputs and outputs. Thus, the following main features of the model are ensured:

- It has a relatively low complexity while faithfully capturing the essential plant dynamics and its nonlinearities over a wide operating range.
- The model is control-oriented in that the manipulated variables, the controlled variables, and the significant disturbances are explicitly shown.
- The model is realistic since constraints on the manipulated variables are considered.

Table 3 includes the ranges of the input variables accepted by the system block shown in Fig. 2. Note that the influence of the inlet pressures of the secondary fluids have not been studied, since their values only affect the calculation of the thermodynamic properties and they are not expected to change appreciably in a real application. The system is ready to be controlled with a sampling period equal or greater than 1 s, starting always at the same operating point described in Table 4.

Table 3. Input variable ranges

Input variable		Range	Unit
Manipulated variables	A_v	[10 – 100]	%
	N	[30 – 50]	Hz
Disturbances	$T_{c,sec,in}$	[27 – 33]	°C
	$\dot{m}_{c,sec}$	[125 – 175]	g · s^{-1}
	$P_{c,sec,in}$	–	bar
	$T_{e,sec,in}$	[-22 – -18]	°C
	$\dot{m}_{e,sec}$	[55 – 75]	g · s^{-1}
	$P_{e,sec,in}$	–	bar
	T_{surr}	[20 – 30]	°C

Table 4. Initial operating point

Variable		Value	Unit
Manipulated variables	A_v	≅ 48.79	%
	N	≅ 36.45	Hz
Disturbances	$T_{c,sec,in}$	30	°C
	$\dot{m}_{c,sec}$	150	g · s^{-1}
	$P_{c,sec,in}$	1	bar
	$T_{e,sec,in}$	-20	°C
	$\dot{m}_{e,sec}$	64.503	g · s^{-1}
	$P_{e,sec,in}$	1	bar
	T_{surr}	25	°C
Output variables	$T_{e,sec,out}$	≅ -22.15	°C
	T_{SH}	≅ 14.65	°C

3. TESTING MULTIVARIABLE CONTROLLERS

The Refrigeration Control System provided within the Benchmark PID 2018 is ready to test any multivariable control strategy. The MATLAB® program called *RS_simulation_management.m* helps to perform this test by automating the simulation execution, data logging, and relevant data representation.

A standard simulation, starting at the operating point described in Table 4, has been scheduled. As shown in Fig. 3, this simulation includes step changes in the references on $T_{e,sec,out}$ and T_{SH}, as well as in the most important disturbances: the inlet temperature of the evaporator secondary fluid $T_{e,sec,in}$ and the inlet temperature of the condenser secondary fluid $T_{c,sec,in}$.

It is observed in Fig. 3 that, although the reference on $T_{e,sec,out}$ does not vary from minute 2, the reference on T_{SH} is changed when applying changes in the disturbances. It is a special feature of the refrigeration systems, which is not exactly a MIMO process with independent variables (Ruz et al., 2017). Fig. 4 shows a variety of steady-state points in the space of the controlled variables. These points have been obtained imposing values all over the range of the manipulated variables (see Table 3), with

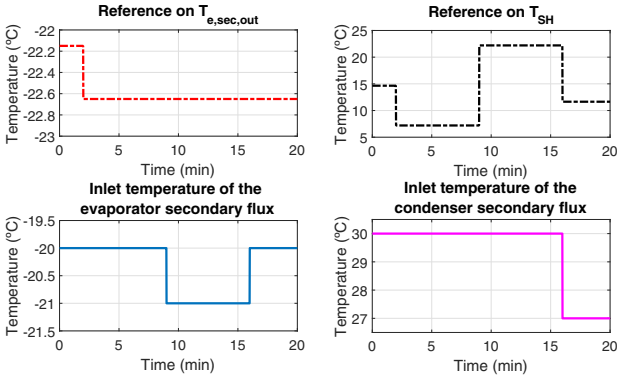

Fig. 3. The standard simulation generates changes in the references on $T_{e,sec,out}$ and T_{SH}, as well as in two disturbance variables: $T_{e,sec,in}$ and $T_{c,sec,in}$

a standard increment of 5% for A_v, and 5 Hz for N, while simultaneously considering the maximum, the minimum, and nominal values of the disturbance $T_{c,sec,in}$, indicated in Tables 3 and 4. It is observed in Fig. 4 that for a given desired value of $T_{e,sec,out}$, there exists a specific range of achievable T_{SH}, thus the reference on T_{SH} cannot be set regardless of the set point on $T_{e,sec,out}$. Furthermore, the range of achievable T_{SH} is expected to vary for different values of the disturbances; this is why the reference on T_{SH} is not only altered when varying the set point on $T_{e,sec,out}$, but also when the disturbances are modified.

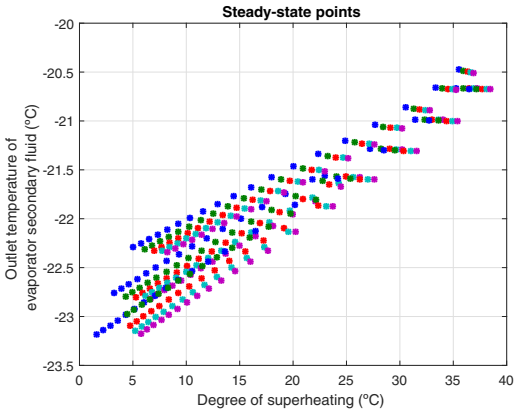

Fig. 4. Steady-state map in the space of the controlled variables, for three values within the range of $T_{c,sec,in}$

The reference and disturbance profiles included in Fig. 3 allow to explore some operating points of the refrigeration system, but any other profiles can be scheduled, considering the ranges expressed in Table 3. Fig. 5 and 6 show the results of the standard simulation using the default controller described in subsection 2.2. The MATLAB® program *RS_simulation_management.m* also generates other figures where some interesting cycle variables are shown, such as the refrigerant pressures, thermal powers, refrigerant mass flow, and the COP, among others.

4. COMPARING MULTIVARIABLE CONTROLLERS

The Benchmark PID 2018 also facilitates the qualitative and quantitative comparison of two controllers based on the same simulation. Fig. 7 and 8 show an example of

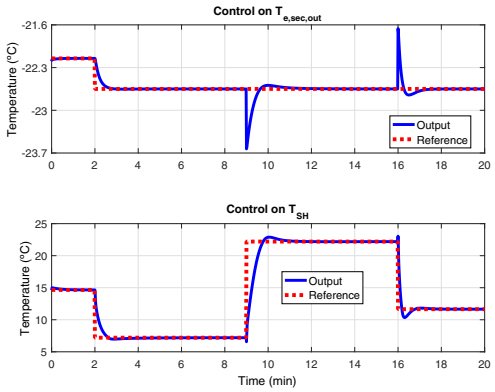

Fig. 5. Example of the standard simulation with the MIMO Refrigeration Control System: controlled variables

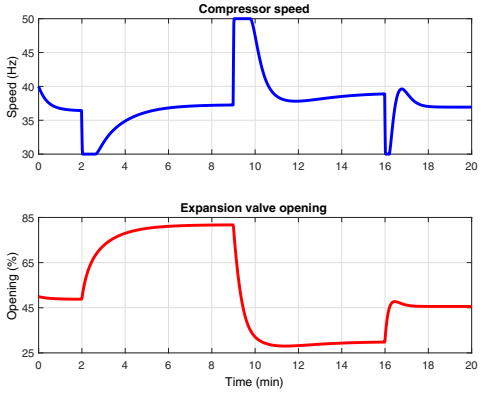

Fig. 6. Example of the standard simulation with the MIMO Refrigeration Control System: manipulated variables

the qualitative comparison. A multivariable PID controller (labelled as *Controller 2* in the figures and as C_2 in the equations) is compared with the default controller described in subsection 2.2 (labelled as *Controller 1*, C_1). The multivariable PID controller is based on the default controller, but it has been designed imposing harder specifications on the closed-loop behaviour. This qualitative example can be checked by calling the MATLAB® function *RS_qualitative_comparison.p* with the names of the two data files as input arguments. This function also generates other comparative figures regarding the refrigerant pressures and mass flow, the thermal powers, and the COP.

Regarding the quantitative comparison, one of the control strategies plays the role of controller of reference (for example the labelled *Controller 1* in Fig. 7 and 8), while the other one plays the role of controller to evaluate (labelled as *Controller 2*). Eight individual performance indices and one combined index are evaluated. The first two indices are the Ratios of Integral Absolute Error ($RIAE$) (Hägglund, 1995), taking into account that both controlled variables should follow their respective references. The third is the Ratio of Integral Time-weighted Absolute Error ($RITAE$) for $T_{e,sec,out}$, considering that the standard simulation only includes one step change in its reference. The fourth, fifth, and sixth indices are the Ratios of Integral Time-weighted Absolute Error ($RITAE$) for T_{SH}, taking into account that the standard simulation includes three step

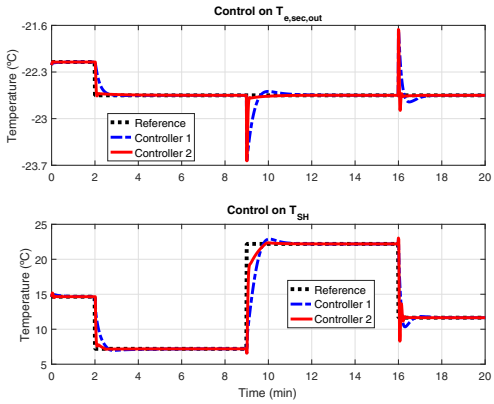

Fig. 7. Example of qualitative comparison of two standard simulations with the MIMO Refrigeration Control System: controlled variables

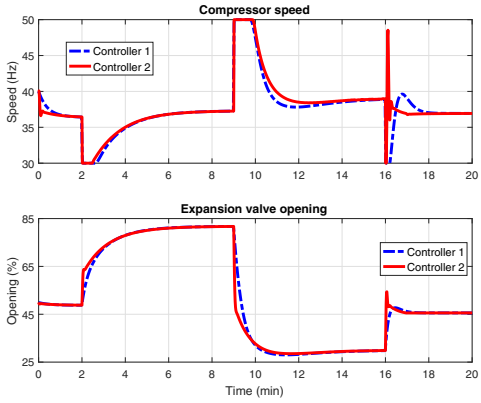

Fig. 8. Example of qualitative comparison of two standard simulations with the MIMO Refrigeration Control System: manipulated variables

changes in its reference. The seventh and eighth indices are the Ratios of Integral Absolute Variation of Control signal ($RIAVU$) for the two manipulated variables. The combined index is obtained as the mean value of the eight individual indices using a certain weighting factor for each index. Equations (1)-(7), which summarise these indices, have been programmed in the MATLAB® function *RS_quantitative_comparison.p*, while the indices associated to the qualitative comparison represented in Fig. 7 and 8 are indicated in Table 5. t_c denotes the corresponding initial step time while t_s refers to the supposed worst-case settling time.

$$IAE_i = \int_0^{time} |e_i(t)|\, dt \tag{1}$$

$$ITAE_i = \int_{t_c}^{t_c+t_s} (t - t_c)\, |e_i(t)|\, dt \tag{2}$$

$$IAVU_i = \int_0^{time} \left| \frac{d\, u_i(t)}{dt} \right| dt \tag{3}$$

$$RIAE_i(C_2, C_1) = \frac{IAE_i(C_2)}{IAE_i(C_1)} \tag{4}$$

$$RITAE_i(C_2, C_1, t_c, t_s) = \frac{ITAE_i(C_2, t_c, t_s)}{ITAE_i(C_1, t_c, t_s)} \quad (5)$$

$$RIAVU_i(C_2, C_1) = \frac{IAVU_i(C_2)}{IAVU_i(C_1)} \quad (6)$$

$$\begin{aligned} J(C_2, C_1) = \frac{1}{\sum_1^8 w_i} \Big[& w_1\ RIAE_1(C_2, C_1) + \\ & + w_2\ RIAE_2(C_2, C_1) + \\ & + w_3\ RITAE_1(C_2, C_1, t_{c1}, t_{s1}) + \\ & + w_4\ RITAE_2(C_2, C_1, t_{c2}, t_{s2}) + \\ & + w_5\ RITAE_2(C_2, C_1, t_{c3}, t_{s3}) + \\ & + w_6\ RITAE_2(C_2, C_1, t_{c4}, t_{s4}) + \\ & + w_7\ RIAVU_1(C_2, C_1) + \\ & + w_8\ RIAVU_2(C_2, C_1) \Big] \end{aligned} \quad (7)$$

Table 5. Relative indices and combined index related to Fig. 7 and 8

Index	Value
$RIAE_1(C_2, C_1)$	0.3511
$RIAE_2(C_2, C_1)$	0.4458
$RITAE_1(C_2, C_1, t_{c1}, t_{s1})$	1.6104
$RITAE_2(C_2, C_1, t_{c2}, t_{s2})$	0.1830
$RITAE_2(C_2, C_1, t_{c3}, t_{s3})$	0.3196
$RITAE_2(C_2, C_1, t_{c4}, t_{s4})$	0.1280
$RIAVU_1(C_2, C_1)$	1.1283
$RIAVU_2(C_2, C_1)$	1.3739
$J(C_2, C_1)$	0.68209

As shown in Fig. 7, *Controller 2* achieves tighter control than *Controller 1*, specially regarding the disturbance rejection, which is reflected in almost all relative indices shown in Table 5. However, the control effort in *Controller 2* is higher, as shown in Fig. 8, thus the relative indices $RIAVU_1$ and $RIAVU_2$ are greater than one. Considering the index weighting, the overall performance of *Controller 2* yields to a better combined index J.

5. CONCLUSIONS

The Benchmark provides a practical approach to the one-compression stage, one-load-demand refrigeration system so that researchers can test their recent developments in the design of PID controllers. It also provides individual and combined performance indices to be used in the comparative evaluation of control strategies. Both multivariable and decentralised PID controllers have been tested and compared using the Simulink® models and the programmed MATLAB® functions of the Benchmark. Nevertheless, its application is not limited to PID controllers, but it allows the test of any multivariable strategy, also at different operating points and control scenarios.

REFERENCES

Alleyne, A. et al. (2012). THERMOSYS 4 Toolbox, University of Illinois at Urbana-Champaign, USA. URL `http://www.thermosys.us`.

Bejarano, G., Alfaya, J.A., Ortega, M.G., and Vargas, M. (2017). On the difficulty of globally optimally controlling refrigeration systems. *Appl. Therm. Eng.*, 111, 1143–1157. doi:10.1016/j.applthermaleng.2016.10.007.

Bejarano, G., Alfaya, J.A., Ortega, M.G., and Rubio, F.R. (2015). Multivariable analysis and H_∞ control of a one-stage refrigeration cycle. *Appl. Therm. Eng.*, 91, 1156–1167. doi:10.1016/j.applthermaleng.2015.09.003.

Hägglund, T. (1995). A control-loop performance monitor. *Control Engineering Practice*, 3(11), 1543–1551.

Jahangeer, K.A., Tay, A.A.O., and Islam, M.R. (2011). Numerical investigation of transfer coefficients of an evaporatively-cooled condenser. *Appl. Therm. Eng.*, 31(10), 1655–1663. doi:10.1016/j.applthermaleng.2011.02.007.

Kalkan, N., Young, E.A., and Celiktas, A. (2012). Solar thermal air conditioning technology reducing the footprint of solar thermal air conditioning. *Renew. and Sustain. Energy Rev.*, 16(8), 6352–6383. doi:10.1016/j.rser.2012.07.014.

Larsen, L.F., Izadi-Zamanabadi, R., and Wisniewski, R. (2007). Supermarket refrigeration system-benchmark for hybrid system control. In *Control Conf. (ECC), 2007 Eur.*, 113–120. IEEE.

Li, B. and Alleyne, A.G. (2010). A dynamic model of a vapor compression cycle with shut-down and start-up operations. *Int. J. of Refrig.*, 33(3), 538–552. doi::10.1016/j.ijrefrig.2009.09.011.

Lukic, R. (2016). Analysis of energy costs in retail trade. *Manag. Res. and Pract.*, 8(4), 5–28.

MacArthur, J.W., Meixel, G.D., and Shen, L.S. (1983). Application of numerical methods for predicting energy transport in earth contact systems. *Appl. Energy*, 13(2), 121–156. doi:10.1016/0306-2619(83)90005-3.

Marcinichen, J., del Holanda, T., and Melo, C. (2008). A dual SISO controller for a vapor compression refrigeration system. In *12th Int. Refrig. and Air Cond. Conf., at Purdue, West Lafayette-IN, USA*.

Rasmussen, H. and Larsen, L.F.S. (2011). Non-linear and adaptive control of a refrigeration system. *IET Control Theory Appl.*, 5(2), 365–378. doi:10.1049/iet-cta.2009.0156.

Ricker, N.L. (2010). Predictive hybrid control of the supermarket refrigeration benchmark process. *Control Eng. Pract.*, 18(6), 608–617. doi:10.1016/j.conengprac.2010.02.016.

Ruz, M.L., Garrido, J., Vázquez, F., and Morilla, F. (2017). A hybrid modeling approach for steady-state optimal operation of vapor compression refrigeration cycles. *Appl. Therm. Eng.*, 120, 74–87. doi:10.1016/j.applthermaleng.2017.03.103.

Salazar, M. and Méndez, F. (2014). PID control for a single-stage transcritical CO_2 refrigeration cycle. *Appl. Therm. Eng.*, 67(1), 429–438. doi:10.1016/j.applthermaleng.2014.03.052.

Schurt, L.C., Hermes, C.J.L., and Trofino-Neto, A. (2009). A model-driven multivariable controller for vapor compression refrigeration systems. *Int. J. of Refrig.*, 32(7), 1672–1682. doi:10.1016/j.ijrefrig.2009.04.004.

Shen, Y., Cai, W.J., and Li, S. (2010). Normalized decoupling control for high-dimensional MIMO processes for application in room temperature control HVAC systems. *Control Eng. Pract.*, 18(6), 652–664. doi:10.1016/j.conengprac.2010.03.006.